Neuroscience Research xxx (xxxx) xxx

Contents lists available at ScienceDirect

Neuroscience Research

journal homepage: www.sciencedirect.com/journal/neuroscience-research

Analysis of splicing abnormalities in the white matter of myotonic dystrophy type 1 brain using RNA sequencing

Kazuki Yoshizumi [a], Masamitsu Nishi [a], Masataka Igeta [b], Masayuki Nakamori [c], Kimiko Inoue [d], Tsuyoshi Matsumura [d], Harutoshi Fujimura [d], Kenji Jinnai [e], Takashi Kimura [a,*]

[a] Department of Neurology, Hyogo Medical University, Nishinomiya, 663-8501 Hyogo, Japan
[b] Department of Biostatistics, Hyogo Medical University, Nishinomiya, 663-8501 Hyogo, Japan
[c] Department of Neurology, Yamaguchi University Graduate School of Medicine, Yamaguchi, 755-8505 Yamaguchi, Japan
[d] Department of Neurology, National Hospital Organization Osaka Toneyama Medical Center, Toyonaka, 560-8552 Osaka, Japan
[e] Department of Neurology, National Hospital Organization Hyogo-Chuo Hospital, Sanda, 669-1515 Hyogo, Japan

ARTICLE INFO

Keywords:
Aberrant splicing
CTG repeats
Gray matter
Muscleblind-like protein
RNA-binding proteins
Glial cell RNAs

ABSTRACT

Myotonic dystrophy type 1 (DM1) is a neuromuscular disorder caused by the genomic expansion of CTG repeats, in which RNA-binding proteins, such as muscleblind-like protein, are sequestered in the nucleus, and abnormal splicing is observed in various genes. Although abnormal splicing occurs in the brains of patients with DM1, its relation to central nervous system symptoms is unknown. Several imaging studies have indicated substantial white matter defects in patients with DM1. Here, we performed RNA sequencing and analysis of CTG repeat lengths in the frontal lobe of patients with DM1, separating the gray matter and white matter, to investigate splicing abnormalities in the DM1 brain, especially in the white matter. Several genes showed similar levels of splicing abnormalities in both gray and white matter, with an observable trend toward an increased number of repeats in the gray matter. These findings suggest that white matter defects in DM1 stem from aberrant RNA splicing in both gray and white matter. Notably, several of the genes displaying abnormal splicing are recognized as being dominantly expressed in astrocytes and oligodendrocytes, leading us to hypothesize that splicing defects in the white matter may be attributed to abnormal RNA splicing in glial cells.

1. Introduction

Myotonic dystrophy type 1 (DM1) is the most common type of muscular dystrophy observed in adults. Patients with DM1 have systemic symptoms including skeletal muscle weakness, cardiac conduction defects, cataracts, glucose intolerance, and central nervous system (CNS) dysfunction. Several neurological symptoms, including cognitive impairment, depression, anxiety, and behavioral disorders have been observed, indicating cerebral involvement (Meola and Cardani, 2015). CNS disorders in patients with DM1 result in decreased quality of life (Bugiardini et al., 2014) and significantly increased disease burden. DM1 is caused by abnormal expansion of CTG-trinucleotide repeats in the 3′ untranslated region (UTR) of the *myotonic dystrophy protein kinase* (DMPK) gene (Brook et al., 1992). The accumulation of toxic RNAs in the nucleus is caused by mutant CTG repeats in the 3′ UTR of DMPK, which inhibits RNA-binding proteins, causing sequestration of muscleblind-like (MBNL) proteins (Mankodi et al., 2001; Miller et al., 2000) and upregulation of CUGBP/Elav-like family proteins (López-Martínez et al., 2020). The sequestration of these proteins affects the alternative splicing (AS) of various genes (Kanadia et al., 2003). We previously identified several splicing abnormalities in the brains of MBNL1/2 knockout mice and patients with DM1, demonstrating that the major splicing factor in the brain is MBNL2 and that MBNL1 functions similarly in the skeletal muscles (Charizanis et al., 2012; Suenaga et al., 2012). Moreover, combined depletion of MBNL proteins by CUG repeats has been a critical factor in the pathogenesis of DM1 in both the brain

Abbreviations: ALS, amyotrophic lateral sclerosis; AS, alternative splicing; CNS, central nervous system; DM1, myotonic dystrophy type 1; DMPK, *myotonic dystrophy protein kinase*; GM, gray matter; MBNL, muscleblind-like; NCBI, National Center for Biotechnology Information; nTPM, transcripts per million; PSI, percent spliced in parameter; qPCR, quantitative polymerase chain reaction; RIN, RNA integrity number; RNA-seq, RNA sequencing; RT, reverse transcriptase; UTR, untranslated region; WM, white matter.

* Corresponding author.
E-mail address: kimura@hyo-med.ac.jp (T. Kimura).

https://doi.org/10.1016/j.neures.2023.10.002
Received 24 February 2023; Received in revised form 3 October 2023; Accepted 5 October 2023
Available online 6 October 2023

and skeletal muscle (Goodwin et al., 2015).

In an earlier study, we investigated splicing abnormalities in patients with DM1 based on the brain region and found less mis-splicing in the cerebellum than that observed in other regions (Nishi et al., 2020; Suenaga et al., 2012).

Mills et al. employed RNA sequencing (RNA-seq) to demonstrate that the gray matter (GM) and white matter (WM) of the human frontal lobe show different transcriptome profiles and distinct AS (Mills et al., 2013). Neuroimaging analyses of the brains of patients with DM1 showed abnormalities in both the GM and WM (Minnerop et al., 2018). Conventional magnetic resonance imaging has demonstrated abnormalities in both the GM and WM, including reduced GM volume (Okkersen et al., 2017), WM hyperintense lesions (Romeo et al., 2010), and anterior temporal WM lesions (ATWML) (Minnerop et al., 2018). Moreover, voxel-based morphometry revealed significantly lower GM and WM volumes in patients with DM1 than in the controls (Antonini et al., 2004). Diffusion tensor imaging studies have revealed a nearly symmetrical reduction of fractional anisotropy in the major association, commissural, and projection fiber tracts, suggesting extensive WM defects (Okkersen et al., 2017).

Considering the extensive damage to the GM and WM in the images, we examined whether the splicing regulation of several genes varied between the GM and WM and found significantly more splicing changes in the GM than in the WM (Nishi et al., 2020). However, only 15 genes were analyzed in this study. Additionally, transcriptome analysis of the frontal cortex of the DM1 brain, using RNA-seq, revealed new splicing abnormalities in genes, such as *GRIP1* (Otero et al., 2021). In this case, transcriptome analysis was only performed for the GM; therefore, a comprehensive survey of splicing abnormalities in the GM and WM is necessary.

We aimed to thoroughly investigate the splicing patterns in the GM and WM using RNA-seq to identify WM-specific splicing abnormalities in this study.

2. Materials and methods

2.1. Ethics and written informed consent

This study was approved by the Ethics Committee of Hyogo Medical University (Approval No. 93), and written informed consent was obtained from the patients or their families for autopsies.

2.2. Pathological analysis

We used brain samples obtained during autopsies from five patients diagnosed with DM1 and five patients with amyotrophic lateral sclerosis (ALS) as a disease control group. The brains were fixed in buffered 10% formalin, embedded in paraffin, and prepared for routine examination with hematoxylin and eosin (H&E) staining. Tissue samples were collected from specific regions, including the anterior part of the cingulate gyrus, the middle frontal gyrus, the primary motor cortex, and the middle temporal gyrus. Immunohistochemical stains were performed on the selected sections using an anti-human PHF-tau antibody (mouse monoclonal, clone AT8 IGH135, Cosmo Bio, Japan; 1:800). The degree of neuronal loss and gliosis was semi-quantitatively evaluated in the selected four aforementioned areas using the following rating scale: 0 for no histopathological alteration; 1 for slight neuronal loss and gliosis; 2 for moderate neuronal loss and gliosis; and 3 for severe neuronal loss and gliosis with tissue rarefaction in the regions. Histopathology of Alzheimer's disease was assessed based on the Braak stage (Braak and Braak, 1991). To visualize the positive immunoreactions, we used a Ventana automated immunostaining instrument (Ventana BenchMark GX, Roche, Switzerland).

2.3. Human RNA collection

RNA was extracted from the right middle frontal gyrus of autopsied brain samples. The brain tissue was sectioned into 60-μm thick sections using a Leica® CM1520 Cryostat (Leica Biosystems, Germany). The boundary between the GM and WM was visually determined, and the tissue was manually separated into the GM and WM. RNA was isolated using RNeasy® Plus Mini (QIAGEN®, Germany).

To confirm the separation of the GM and WM, we performed quantitative reverse transcription (RT) polymerase chain reaction (PCR) (qPCR), using primers for *NEFH* (expressed to a higher level in the GM), *MOG* (expressed to a higher level in the WM), and *GAPDH* (control) (Mills et al., 2013) (Table 1), with PowerUp™ SYBR™ using the Thermal Cycler Dice® Real Time System III (TAKARA Bio, Japan). These PCRs were run in triplicate, and the expression levels of *NEFH* and *MOG* were calculated using the 2-ΔΔCt method with GAPDH as a control; the data are shown as the mean of the triplicates.

2.4. RNA-seq analysis

The RNA quality was assessed using an Agilent 2100 Bioanalyser (Agilent Technologies, USA). Three samples each of ALS and DM1 were selected for RNA-seq, and their RNA integrity number (RIN) values were > 6.5, whereas the RIN values of the remaining two ALS and DM1 were > 3.0. RNA-seq was performed using DNBSEQ-G400 (MGI Tech, Co., Ltd, China) at BGI Genomics and sequenced to a depth of approximately 40 million read pairs. The read quality was assessed using fastQC (version 0.11.9). The reads were aligned to the human reference genome (GRCh38) using HISAT2 (version 2.0.4) (Kim et al., 2015). The aligned and sorted bam files were used for AS analysis using rMATS (version 4.1.2) (Shen et al., 2014). We calculated the percent spliced in parameter (PSI), denoted as the ratio of alternative exons, using the RNA-seq results.

2.5. Establishing criteria for abnormal splicing

The AS events were identified using the following criteria: a false discovery ratio of ≤ 0.05, inclusion and exclusion reads ≥ 20, P value < 0.01 using a likelihood-ratio test, and an average level of PSI (ΔPSI) ≥ 0.2.

2.6. Primer design

Based on the RNA-seq results, the DNA sequences of the splicing events were identified using Genetyx®-Network version 16.0.1 (Genetyx Corporation, Japan) and the National Center for Biotechnology Information (NCBI) database. Eight candidate splicing events were abnormal only in the WM, and three were abnormal in both the GM and WM. One of them was *ADD1* exon 8, which was examined in our previous study (Nishi et al., 2020). Ten mis-spliced exons were identified, including *ASPDH* exon 5 (150 nt.), *CACNA1A* exon 45 (36 nt.), *DNM1* exon 22 (37 nt.), *GPM6A* exon 2 (59 nt.), *IP6K2* exon 2 (139 nt.), *MBD1* exon 9 (75 nt.), *NPRL3* exon 5 (75 nt.), *PALM* exon 8 (132 nt.), *PLPP1* exon 3 (155 nt.), and *ZFYVE21* exon 6 (54 nt.). Forward and reverse primers were designed for each splicing gene using NCBI Primer-BLAST (https://www.ncbi.nlm.nih.gov/tools/primer-blast/) and Primer3 (https://bioinfo.ut.ee/primer3–0.4.0/) (Table 2).

Table 1
Sequence of primers created for confirmation of separation with reverse transcription quantitative polymerase chain reaction.

Genes	Forward primer	Reverse primer
NEFH	AGGTGAAGAGTGTCGGATTG	GAAGCGAGAAAGGAATTGGG
MOG	CCTCCACTTGGCCTGACCTT	ACCTCCATGCCTGTAGCGTT
GAPDH	CCATCACTGCCACCCAGAAGAC	CCATCACGCCACAGTTTCCC

Table 2
Sequence of primers created for validation of mis-splicing with reverse transcription polymerase chain reaction.

Genes (target exon)	Forward primer	Reverse primer
ASPDH (exon 5 [150 nt.])	GAATCTGGGGCACAAATCCT	CATGGTGACACGAAGGCT
CACNA1A (exon 45 [36 nt.])	TAACTCTCAGTCCGTGGAGATG	TCCAGCGAGTAATCGTCCAG
DNM1 (exon 22 [37 nt.])	ATCATCGGCGACATCAACAC	TCTCAGGACGGGATGGACTT
GPM6A (exon 2 [59 nt.])	ACTGCAGAGAAGCAGGACCTC	GTTCAGCTCAGTAGATTCGCAC
IP6K2 (exon 2 [139 nt.])	AACAATAGGACGGAAACGCC	TGTTGTTTGTCCGTGTGTCC
MBD1 (exon 9 [75 nt.])	TCAGACCCAAGAGGATTGTG	AGCCATCTTGGAGTCACAGC
NPRL3 (exon 5 [75 nt.])	CCAAGTCTGAAATGTGTGGC	CAGACAGTTTATCACTGACGGG
PALM (exon 8 [132 nt.])	CAGGACGACGAGCAGAAGAC	GATGAGTTCGTCCACCTCGG
PLPP1 (exon 3 [155 nt.])	AGCTCAGTCCATCGCCCTT	TGACTAGCAGCTGCACCAAA
ZFYVE21 (exon 6 [54 nt.])	CGTCACGTTTGGAAACTCAG	TGTATACTGCAGGAACATGCC

2.7. RT-PCR methods

We used random hexamers with the SuperScript® III First-Strand Synthesis System (Invitrogen™, USA) in accordance with the manufacturer's instructions and synthesized cDNA from 400 ng of extracted of RNA. AmpliTaq Gold® 360 Master Mix (Applied Biosystems, USA) was used to amplify cDNA with primers under the following PCR conditions: 94 °C for 4 min, 36 cycles of 94 °C for 30 s, 61 °C for 30 s, and 72 °C for 1 min. In a previous study, 400 ng of RNA was used in RT-PCR, and the number of cycles was set to 36 after confirming the linearity of PCR amplification in each cycle (Nishi et al., 2020). In this study, 400 ng of RNA was used as well; thus, the number of RT-PCR cycles was set to 36. We analyzed the PCR products using an Agilent 2100 Bioanalyser.

2.8. Human gene expression profile

The Human Protein Atlas (https://www.proteinatlas.org/) was used to obtain the expression data of genes with dysregulated splicing in both WM and GM. Specifically, the Single Cell Type section provided information on the expression of protein-coding genes in individual human cell types based on scRNA-seq (Table S1, S2). The transcripts per million (nTPM) value for each gene was obtained from this website.

2.9. Human DNA collection

DNAs were extracted from the brains of three patients with DM1 and separated into the GM and WM using the same method as for RNA. We isolated the DNAs by phenol/chloroform extraction and ethanol precipitation as previously described (Thornton et al., 1994).

2.10. Southern blotting

Southern blotting was performed as described by Nakamori et al. (Nakamori et al., 2009) with slight modifications. Genomic DNA was digested using *Hae*III and *Alu*I. The fragments were separated on 0.7% agarose gels buffered with 40 mM Tris-acetate at 4 V/cm for 6 h and transferred overnight to nylon membranes (Roche, Switzerland) by alkaline transfer. After ultraviolet crosslinking, blots were hybridized with 10 pmol/ml DIG-labeled $(CAG)_7$ (5′-gcAgCagcAgca-3′) at 70 °C for 4 h in hybridization buffer (5 × SSC, 1% block solution [Roche, Switzerland], 0.1% N-laurylsarcosine, 0.02% sodium dodecyl sulfate). Blots were washed with high stringency (0.5 × SSC, 70 °C) and developed with alkaline phosphatase-conjugated anti-DIG antibody (Roche, Switzerland) with CDP-Star substrate in accordance with the manufacturer's instructions, followed by chemiluminescence detection using ChemiDoc MP imager (Bio-Rad, USA).

2.11. Statistical analyses

We performed Welch's t-test to test the mean difference in the PSI between ALS and DM1 using a two-sided significance level of 5% for all comparisons. We did not adjust the significance level for multiplicity to maintain the maximum power, as indicated by Saville (Saville, 1990). The ΔPSI was calculated by subtracting the average PSI of the ALS from DM1. We demonstrated the summary statistics, 95% confidence intervals derived from the unpooled variance, and p-values obtained by Welch's t-test for the difference between mean ΔPSI GM and mean ΔPSI WM for each exon as described in a previous study (Nishi et al., 2020).

To compare the extension of CTG repeats in DM1 GM and WM, P-values were obtained using a one-sample t-test from the number of GM repeats minus the number of WM repeats in the same patient. Given the potential non-normal distribution of repeat length data, we also compared GM and WM repeat lengths using the non-parametric Wilcoxon signed rank exact test. These statistical analyses were performed using EZR (Saitama Medical Center, Jichi Medical University, Japan) (Kanda, 2013), which is a graphical user interface for R (The R Foundation for Statistical Computing, Austria). The number of peak repeats was considered the number of CTG repeats.

3. Results

3.1. Clinical, neuroimaging, and pathological characteristics

We demonstrate the clinical (sex, age, onset age, duration, type of DM1, cognitive decline), neuroimaging (magnetic resonance imaging [MRI]), and pathological (neuronal loss in each area, and Braak staging) findings (Tables 3, 4). Most DM1 patients showed neuroimaging abnormalities such as white matter T2 hyperintensities and enlarged lateral ventricle but displayed no or slight neuronal loss and gliosis in pathological analysis. Braak staging ranged from stage I to III.

3.2. Confirmation of separation of the GM and WM

qPCR analysis revealed that the expression levels of *NEFH* were higher in the GM samples, whereas those of *MOG* were higher in the WM samples, verifying that each sample was successfully segregated into GM and WM (Fig. 1).

3.3. Comprehensive study of mis-splicing with RNA-seq

We identified 31 mis-spliced events in the GM, eight events in the WM, and three events in both the GM and WM using our criteria (Fig. 2). These WM events included *PALM* exon 8 and *ZFYVE21* exon 6, which were previously reported to be mis-spliced in the frontal cortex and heart of DM1, respectively (Freyermuth et al., 2016; Otero et al., 2021).

3.4. Validation of mis-splicing with RT-PCR

To validate the splicing abnormalities in the WM, ten splicing events

Table 3
Clinical characteristics and RNA quality of each patient.

Disease	No	Sex	Age (years)	Onset age (years)	Duration (years)	Type of myotonic dystrophy type 1	postmortem time (hours:minutes)	RNA integrity Number grey/white matter	RNA sequence
Myotonic dystrophy type 1	1	M	41	5	36	Juvenile	1:55	7.1/8.5	○
	2	F	58	38	20	Adult onset	1:40	6.5/7.4	○
	3	M	57	18	39	Juvenile	8:20	6.6/7.3	○
	4	M	47	12	35	Juvenile	16:35	4.7/3.3	
	5	M	51	40	11	Adult onset	2:00	6.3/5.9	
Amyotrophic lateral sclerosis	1	M	69	N/A	N/A	N/A	0:47	8.1/7.7	○
	2	F	73	N/A	N/A	N/A	4:52	7.8/8.2	○
	3	F	53	N/A	N/A	N/A	2:24	7.7/8.4	○
	4	F	73	N/A	N/A	N/A	4:04	7.3/8.2	
	5	M	70	N/A	N/A	N/A	18:22	8.6/7.5	

Type of DM1: juvenile onset (age of onset, 10 – 20 years), adult onset (age of onset, 20 – 40 years), and late onset (age of onset > 40 years).

Table 4
Cognitive functions, and imaging and pathological findings of each patient.

Disease	No	Cognitive decline	Brain MRI findings	Pathological findings	
				Braak stage	Neuronal loss
Myotonic dystrophy type 1	1	Mild	white matter hyperintense lesions of frontal lobe	N/A	1
	2	Mild	white matter hyperintense lesions of frontal lobe	Braak I	1
	3	Mild	N/A	Braak II	0
	4	Severe	cortex atrophy and white matter hyperintense lesions of frontal lobe	Braak III	0
	5	Mild	cortex atrophy of frontal lobe	Braak III	0
Amyotrophic lateral sclerosis	1	Normal	no data	Braak II	0
	2	Normal	no data	Braak II	0
	3	Normal	no data	Braak III	0
	4	Normal	no data	Braak III	0
	5	Normal	no data	Braak II	1

The degree of cognitive decline was rated on three levels: normal, mild, and severe.
The degree of neuronal loss and gliosis was semi-quantitatively evaluated in the selected four aforementioned areas using the following rating scale: 0 for no histopathological alteration; 1 for slight neuronal loss and gliosis; 2 for moderate neuronal loss and gliosis; and 3 for severe neuronal loss and gliosis with tissue rarefaction in the regions.

in the WM (excluding *ADD1* exon 8) were examined by RT-PCR in five ALS and five DM1 brains, including three ALS and three DM1 brain samples that were used in the RNA-seq study.

Compared with the ALS brains, the PSIs of *PALM* exon 8, *CACNA1A* exon 45, *ZFYVE21* exon 6, and *MBD1* exon 9 in the GM and WM of the DM1 brains were significantly different, suggesting that these genes are spliced in both the GM and WM of DM1 brains (Fig. 3). When comparing PSIs of ZFYVE21exon 6 and MBD1 exon 9 between GM and WM in both ALS and DM1, higher values were consistently observed in GM than in WM. The PSI of *PLPP1* exon 2 was significantly different in the GM, but not in the WM of DM1 brains compared with ALS brains. The PSI of *DNM1* exon 22 could not be calculated owing to the nonspecific PCR products (data not shown).

Next, ΔPSI was used to compare the extent of mis-splicing of the exons that showed a significant difference between the DM1 and ALS brains and between the GM and WM (Fig. 4). The mean PSIs of *PALM* exon 8 were 29.26% and 36.12% for the GM and WM in ALS brains, respectively, and 4.36% and 9.23% for the GM and WM in DM1 brains, respectively. The ΔPSI of the GM was –24.90%, and that of the WM was –26.89% between the two disorders. The difference in the ΔPSI between DM and ALS (95% confidence intervals) was –1.98%, (–19.282–15.318%), and the P-value was 0.7735. Among all the five examined samples, no significant differences in ΔPSI were found between the GM and WM, suggesting that abnormal splicing of these genes in the GM and WM occurs to the same extent.

To explore if the genes with dysregulated splicing in WM in DM1 were expressed dominantly in a specific cell population, we investigated the expression profile of these genes using a single cell analysis database (The Human Protein Atlas). The expression values reported on the website are shown in Table S1 and S2. Out of four splicing events shown to be at the same level of mis-splicing in the WM as in the GM, *PALM* and *ZFYVE21* are expressed to a greater degree in astrocytes and/or oligodendrocytes than in excitatory and inhibitory neurons. These results suggest that mis-splicing of these genes in astrocytes and oligodendrocytes in the WM may contribute to DM1 pathogenesis.

3.5. Comparison of the CTG repeat lengths in the GM and the WM of DM1

The peak density of the longest band for each sample was estimated based on the expansion size. The number of CTG repeats in each sample was as follows: GM and WM: (1) 2970 and 2370, (2) 3060 and 2890; and (3) 3150 and 2510, respectively (Fig. 5), with no statistically significant difference between GM and WM ($P = 0.089$, one-sample t-test; $P = 0.25$, Wilcoxon signed rank exact test). However, the number of repeats in the GM tended to be extended in all the samples.

4. Discussion

Otero et al. reported 130 high-confidence splicing events in the frontal cortex of DM1 brains (Otero et al., 2021). In contrast, we performed RNA-seq on both GM (cortex) and WM tissue samples from the brains of patients with DM1. We found 31 mis-spliced events limited to GM, eight mis-splicing events limited to WM, and three mis-splicing events in both GM and WM. Among these events, four (*PLA2G6*, *GABRG2*, *PACS2*, *CSNK1D*), two (*IP6K2* and *MBD1*), and two events (*ADD1* and *PALM*), respectively, were also reported in Otero's study (Table S1, S2).

Although RT-PCR validation did not reveal any genes causing abnormal splicing in the WM only, the following genes in the WM showed the same level of mis-splicing as in the GM: *PALM* exon 8, *CACNA1A* exon 45, *ZFYVE21* exon 6, and *MBD1* exon 9. In this study, the PSIs of certain genes, such as MBD1 and ZFYVE21, differed between

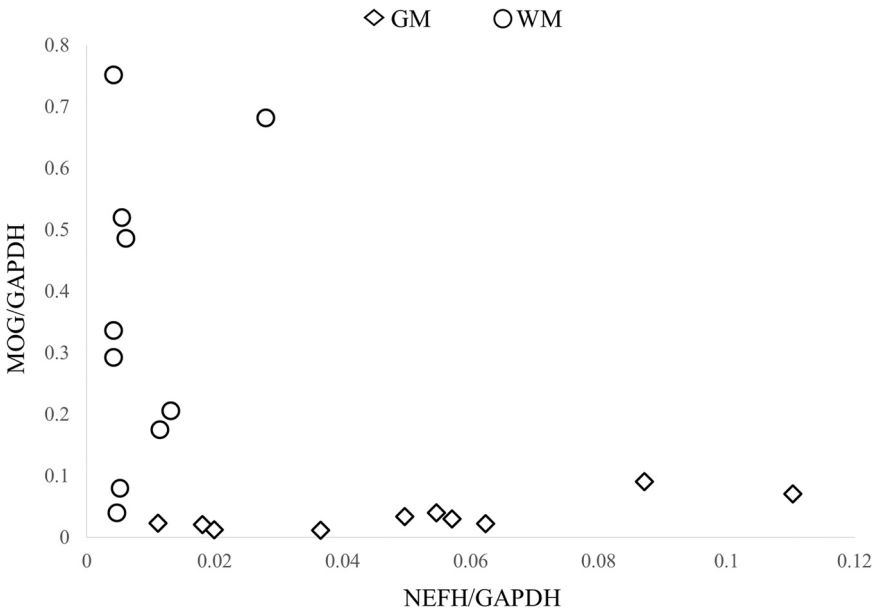

Fig. 1. Comparison of the *NEFH* and *MOG* expression levels in the GM and WM. The expression levels of *NEFH* and *MOG* were calculated using the 2-ΔΔCt method with *GAPDH* as a control, and data are shown as the mean of triplicates. GM, gray matter; WM, white matter.

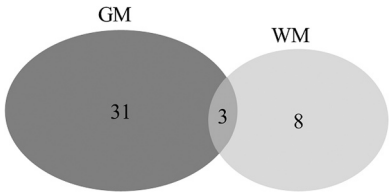

Fig. 2. Number of mis-spliced genes in the GM and WM found by RNA-seq. This Venn diagram shows the number of abnormally spliced exons in the GM and WM of myotonic dystrophy type 1 under the defined criteria. The overlapping areas in the Venn diagram are genes that showed abnormal splicing in both the GM and WM. GM, gray matter; RNA-seq, RNA sequencing; WM, white matter.

GM and WM in both ALS and DM1 (Fig. 3). However, ΔPSI (extent of mis-splicing) between ALS and DM1 did not differ significantly in each region (Fig. 4). Of these four genes, three (*MBD1* exon 9, *CACNA1A* exon 45, and *PALM* exon 8) have been reported as being in the top 130 high-confidence splicing events by (Otero et al., 2021). These three previously reported genes, plus one newly identified gene, *ZFYVE21* exon 6, were mis-spliced to the same extent in the WM. Therefore, we suggest that these splicing changes might be related to substantial WM damage in DM1 brains.

We previously examined the differences in the splicing regulation of several genes between the GM and WM and reported significantly more splicing abnormalities in the GM than in the WM. In seven of the 15 genes examined, the extent of splicing change between DM1 and ALS in the GM was significantly higher than that detected in the WM. In contrast, none of the genes showed a significant increase in the extent of splicing in the WM versus the GM.

The results of RNA-seq and RT-PCR revealed four new genes, *PALM* exon 8, *MBD1* exon 9, *CACNA1A* exon 45, and *ZFYVE21* exon 6, which showed significant abnormal splicing in the WM.

PALM localizes to axons, the plasma membranes of postsynaptic specializations, and dendritic processes. AS of *PALM* exon 8 modulates the reduction in synapse formation, filopodia induction and AMPA receptor recruitment (Arstikaitis et al., 2008). These changes are associated with alterations in synaptic and structural plasticity, including the induction of long-term potentiation. *MBD1* is involved in epigenetic gene regulation via DNA methylation (Jobe and Zhao, 2017). As Mbd1−/− mice exhibit symptoms of reduced social interaction, learning disabilities, anxiety, sensorimotor gating deficits, and depression, *MBD1* can be associated with these symptoms (Allan et al., 2008). Some of these symptoms are similar to the CNS symptoms observed in patients with DM1. However, the effects of AS of *MBD1* exon 9 have not yet been reported.

No previous study has reported on the effects of AS of *CACNA1A* exon 45 and *ZFYVE21* exon 6, both of which were mis-spliced in the GM and WM in this study. The *CACNA1A* gene encodes the P/Q-type voltage-gated Ca2 + channel α1 subunit CaV2.1 and is involved in neurotransmitter release and synaptic plasticity (Mori et al., 1991; Nanou and Catterall, 2018). *CACNA1A* has been associated with episodic ataxia type 2, familial hemiplegic migraine type 1, and spinocerebellar ataxia type 6 (Hommersom et al., 2022). *ZFYVE21* has been a complement inducer of NF-κB in endothelial cells (Fang et al., 2019); however, its function in the nervous system is poorly understood. Mis-splicing of these genes can possibly result in changes in the WM, leading to CNS symptoms.

We have added new insights to our previous discussion of splicing differences between the GM and WM (Nishi et al., 2020) and proposed several explanations for our findings. First, the cell types vary between the GM and WM; neuronal cell bodies, protoplasmic astrocytes, and microglial cells are found primarily in the GM, whereas the WM includes axons, oligodendrocytes, fibrous astrocytes, microglial cells, and ependymal cells. In the DM1 brains, although the effects on non-neuronal cells remain unclear, RNA foci accumulate in the astrocytes, oligodendrocytes, and neurons (Hernández-Hernández et al., 2013; Jiang et al., 2004). Dincă et al. reported that astrocytes in the frontal cortex and hippocampus of mice were affected by CUG-RNA toxicity, and that mis-splicing, which was observed in the astrocytes but not in the neurons, could be related to the functional defects in cell adhesion and spreading (Dincă et al., 2022). Accumulation of RNA foci and splicing abnormalities have also been reported in the oligodendrocytes of mice (González-Barriga et al., 2021). Several mis-splicing events have been found in the WM glial cells of patients with DM1, and some of the mis-splicing events are more prominent in the WM glial cells than in the GM neurons (Nakamori et al., 2022). Thus, splicing abnormalities in the glial cells, such as astrocytes and oligodendrocytes, can be related to the differences in splicing defects between the GM and WM. Indeed, a single-cell-based database (The Human Protein Atlas) demonstrated that

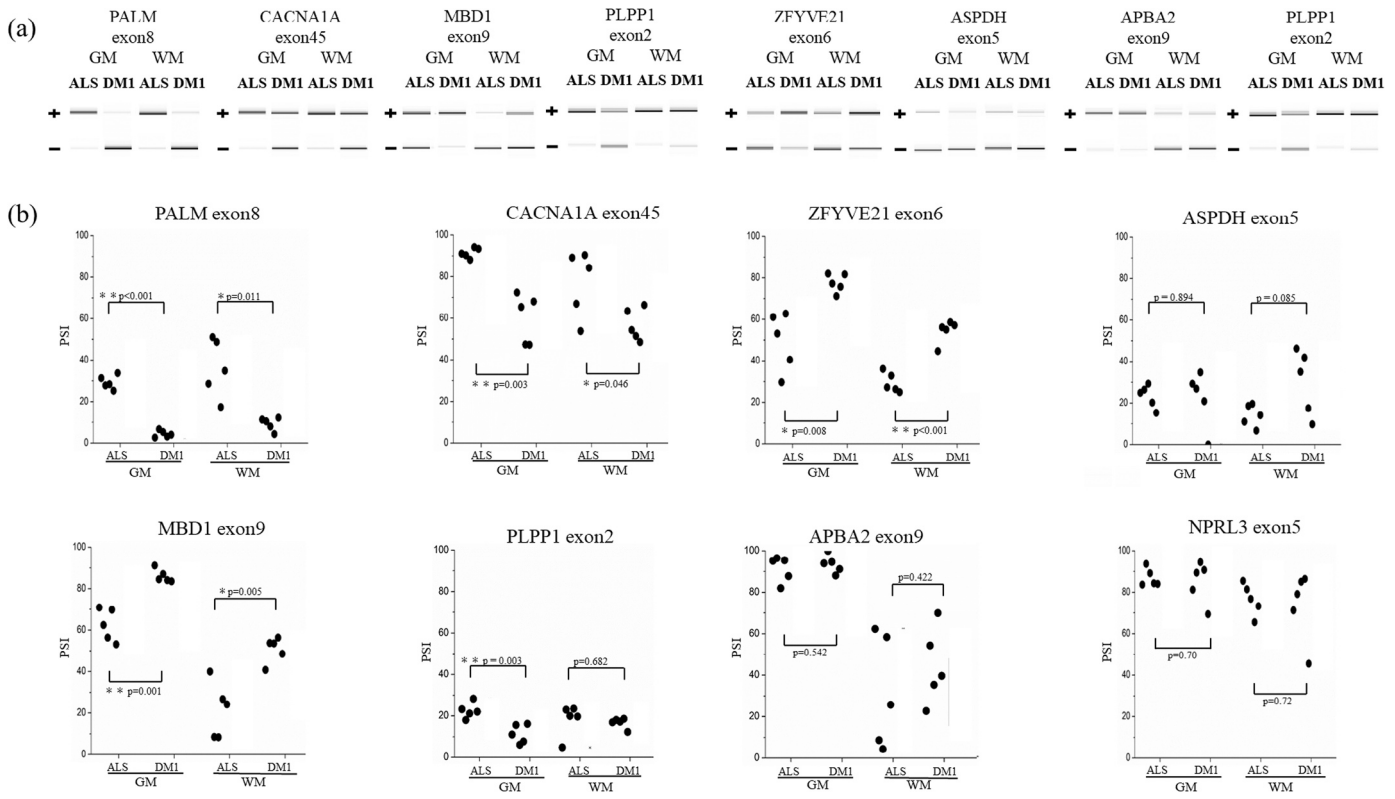

Fig. 3. Validation of mis-splicing by RT-PCR. (a) RT-PCR products from the GM and WM in ALS and DM1. (b) PSI of alternative exons in the GM and WM for candidate genes from RNA-seq results. The PSI values for each gene were analyzed using Welch's t-test. The graph is shown as a box and whisker diagram, with the line in the box representing the median and the square symbol representing the mean. RT-PCR, real-time polymerase chain reaction; PSI, percent spliced in parameter; ALS, amyotrophic lateral sclerosis; DM1, myotonic dystrophy type 1; GM, gray matter; WM, white matter.

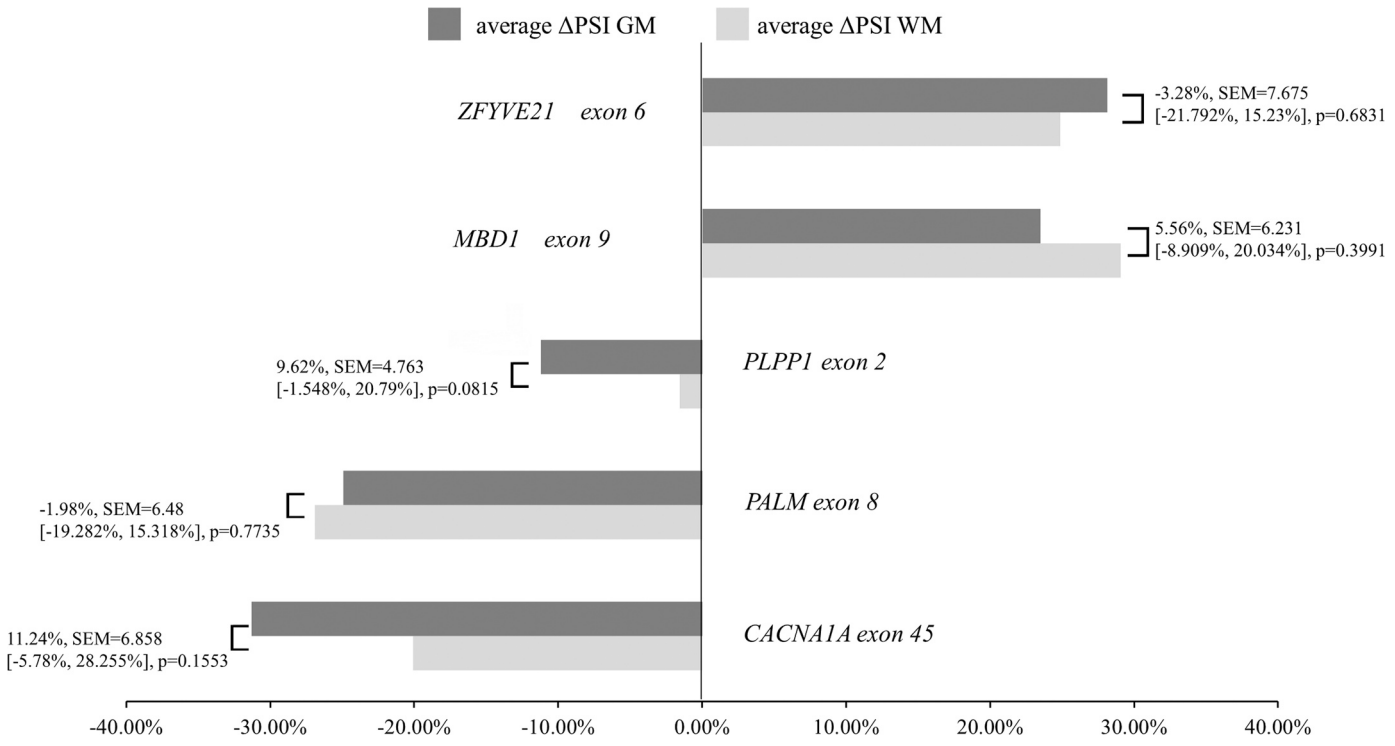

Fig. 4. Comparison of the degree of mis-splicing in the GM and WM using ΔPSI. Bar graph showing a comparison of the mean ΔPSI GM and mean ΔPSI WM of five samples using Welch's t-test for genes that showed mis-splicing in the GM and WM of DM1 brains by RT-PCR. The numbers in the graphs represent the mean difference for comparison of the mean ΔPSI GM and mean ΔPSI WM, SEM (lower CL, upper CL), and P-values in this order. RT-PCR, real-time polymerase chain reaction; PSI, percent spliced in parameter; DM1, myotonic dystrophy type 1; GM, gray matter; WM, white matter.

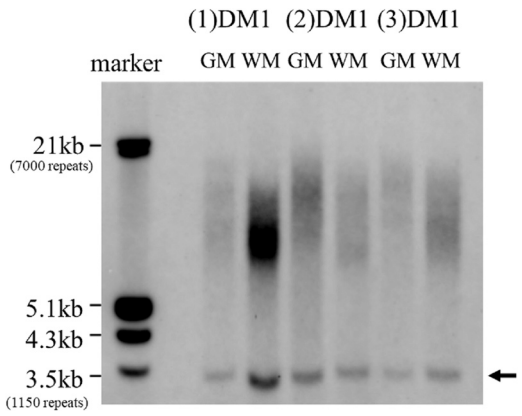

Fig. 5. Southern blot analysis of DNA from the GM and WM in DM1 brains. From the left lane, molecular weight markers, (1) DM1: GM WM, (2) DM1: GM WM, and (3) DM1: GM WM. The arrow indicates nonspecific signal. The peak density of the longest band for each sample was estimated based on the expansion size. The numbers of CTG repeats were as follows (GM and WM): (1) 2970 and 2370, (2) 3060 and 2890, and (3) 3150 and 2510, respectively. DM1, myotonic dystrophy type 1; GM, gray matter; WM, white matter.

two (*PALM* exon 8 and *ZFYVE21* exon 6) out of the four genes with dysregulated splicing in our study are dominantly expressed in astrocytes or oligodendrocyte rather than in excitatory or inhibitory neurons. Thus, functional and subcellular localization experiments would be necessary to elucidate the downstream consequences of mis-splicing of these genes in astrocytes. Second, it is possible that different transcriptional activities in the axons and neuronal cell bodies can possibly affect the distribution of splicing isoforms. Some mRNAs are transcribed by RNA-binding proteins in the neuronal cell body and then transported to the axons (Cioni et al., 2018). Protein synthesis in the axons, termed local protein synthesis, occurs primarily in developing axons and during regeneration of injured axons (Martin, 2004). The distribution of mRNAs in axons was examined using transcriptome analysis (Agrawal and Welshhans, 2021). Axons in early development have a propensity to express mRNAs related to axon extension, whereas those in late development tend to express mRNAs encoding proteins related to dendrites and synapse formation. The selectivity of transported mRNAs can be associated with the splicing differences between the GM and WM. Third, the difference in the number of repeats between the GM and WM can propel abnormal splicing. Certainly, Nakamori et al. measured the CTG repeat length in the neurons of the GM and glial cells of the WM in the anterior temporal lobe and reported that neurons of the GM had significantly longer repeats (Nakamori et al., 2022). In the present study, the number of repeats in the GM and WM was not statistically significantly different; however, the number of repeats in the GM was extended in all the samples. This difference in the number of repeats could explain the differences in splicing.

It remains unclear how differences in splicing between the GM and WM are linked to brain damage. In WM pathology, loss of myelin, widened perivascular spaces in deep and subcortical WM, and loss of axons have been reported. However, some reports have indicated that axons remain relatively intact (Weijs et al., 2021). *PALM* exon 8, which was found to have splicing defects in this study, has been previously reported to be mis-spliced in the astrocytes using a mouse model (González-Barriga et al., 2021), suggesting that differences in the splicing isoforms in glial cells affect the splicing defects between the GM and WM. We had predicted Wallerian degeneration as the cause of this WM damage owing to more abundant splicing abnormalities in the GM. However, based on the results of the current study and the preservation of axons in some cases in pathology, we considered the possibility that the WM disorder of the brain in DM1 was affected by splicing abnormalities in the glial cells, including astrocytes and oligodendrocytes. The genes that were newly identified to be aberrantly spliced in the WM in this study could be related to the WM disorders in the brain of patients with DM1.

This study has some limitations. First, we used ALS brain samples for disease control, which could show splicing changes in the GM and WM (Butti and Patten, 2019). However, we previously compared the splicing between disease controls (seven of nine samples were ALS) and healthy controls and found no significant difference (Charizanis et al., 2012). Second, the sample size used for RNA-seq was limited. As we investigated three samples of each group, variability of mis-splicing among samples may weaken detection sensitivity. As Otero et al. included 21 patients with DM1 in their RNA-seq analysis (Otero et al., 2021), we need to validate these findings using more samples in the future. Third, since we used postmortem frontal lobes in this study, we cannot deny the influence of RNA degradation due to postmortem time. Postmortem time is negatively correlated with RIN values and RNA yield (Gallego Romero et al., 2014). In the study of postmortem time, RIN values, and gene expression in samples used for RNA-seq, the cutoff for RIN values was set between 7.9 and 6.4 as a reference value. In all samples used for RNA-seq in this study, RIN values were higher than this range. We cannot rule out the possibility that RNA degradation may have affected the RNA-seq results. Fourth, our WM samples contained axons and various cells, such as glial cells. Therefore, it may be necessary to isolate individual cells using laser microdissection and perform RNA-seq to account for the heterogeneity of the sample. Finally, differences in cell-type composition between DM1 and disease controls can cause differences in splicing. To avoid this issue, the proportion of each cell type should be estimated using a larger dataset. Additionally, future studies should investigate the accumulation of RNA foci to clarify potential differences between pathological processes in each cell population.

5. Conclusion

In this study, we performed RNA-seq and found several genes that revealed splicing defects in the WM and GM of DM1 brains. Although we did not find any splicing events that exclusively occurred in the WM of DM1 brains, we believe these splicing defects may play a role in WM damage. In particular, abnormal splicing of *PALM* exon 8 has been previously reported in DMXSL mouse astrocytes. These results suggest that splicing abnormalities in the astrocytes and other glial cells may be involved in WM defects in the DM1 brain.

Funding

This work was supported by JSPS KAKENHI (Grant Number: JP18K07515) awarded to TK, as well as by AMED 22wm0425019h0002 awarded to KI and HF. The funding sources were not involved in the study design, data collection, analysis, or interpretation, nor in the writing of the report, and they had no role in the decision to submit the article for publication.

Data Availability

RNA-seq data generated in this study are available in GEO (accession number GSE224437).

Acknowledgements

We thank Editage (www.editage.jp) for the English language editing.

Declarations of interest

None.

Appendix A. Supporting information

Supplementary data associated with this article can be found in the online version at doi:10.1016/j.neures.2023.10.002.

References

Agrawal, M., Welshhans, K., 2021. Local translation across neural development: a focus on radial glial cells, axons, and synaptogenesis. Front. Mol. Neurosci. 14. https://doi.org/10.3389/FNMOL.2021.717170.

Allan, A.M., Liang, X., Luo, Y., Pak, C., Li, X., Szulwach, K.E., Chen, D., Jin, P., Zhao, X., 2008. The loss of methyl-CpG binding protein 1 leads to autism-like behavioral deficits. Hum. Mol. Genet 17, 2047–2057. https://doi.org/10.1093/HMG/DDN102.

Antonini, G., Mainero, C., Romano, A., Giubilei, F., Ceschin, V., Gragnani, F., Marino, S., Fiorelli, M., Soscia, F., di Pasquale, A., Caramia, F., 2004. Cerebral atrophy in myotonic dystrophy: a voxel based morphometric study. J. Neurol. Neurosurg. Psychiatry 75, 1611–1613. https://doi.org/10.1136/JNNP.2003.032417.

Arstikaitis, P., Gauthier-Campbell, C., Herrera, R.C.G., Huang, K., Levinson, J.N., Murphy, T.H., Kilimann, M.W., Sala, C., Colicos, M.A., El-Husseini, A., 2008. Paralemmin-1, a modulator of filopodia induction is required for spine maturation. Mol. Biol. Cell 19, 2026–2038. https://doi.org/10.1091/MBC.E07-08-0802.

Braak, H., Braak, E., 1991. Neuropathological stageing of Alzheimer-related changes. Acta Neuropathol. 82, 239–259. https://doi.org/10.1007/BF00308809.

Brook, J.D., McCurrach, M.E., Harley, H.G., Buckler, A.J., Church, D., Aburatani, H., Hunter, K., Stanton, V.P., Thirion, J.P., Hudson, T., Sohn, R., Zemelman, B., Snell, R. G., Rundle, S.A., Crow, S., Davies, J., Shelbourne, P., Buxton, J., Jones, C., Juvonen, V., Johnson, K., Harper, P.S., Shaw, D.J., Housman, D.E., 1992. Molecular basis of myotonic dystrophy: expansion of a trinucleotide (CTG) repeat at the 3′ end of a transcript encoding a protein kinase family member. Cell 68, 799–808. https://doi.org/10.1016/0092-8674(92)90154-5.

Bugiardini, E., Meola, G., Alvarez, C., Angeard, N., Bassez, G., Day, J.W., Dent, G., Ekström, A.B., Eymard, B., Fossati, B., Gagnon, C., Gomes-Pereira, M., Gourdon, G., Heatwole, C., Housman, D.E., Johnson, N.E., Kornblum, C., MacKenzie, D., Minnerop, M., Morris, C., Nishino, S., Pearson, C.E., Pletcher, M., Ranum, L., Reddy, S., Richer, L., Schoser, B., Sergeant, N., Wang, E., Wentworth, B., Winblad, S., Wozniak, J., Swanson, M.S., Ladd, A., 2014. Consensus on cerebral involvement in myotonic dystrophy: Workshop report: May 24–27, 2013, Ferrere (AT), Italy. Neuromuscular Disorders 24, 445–452. https://doi.org/10.1016/J.NMD.2014.01.013.

Butti, Z., Patten, S.A., 2019. RNA dysregulation in amyotrophic lateral sclerosis. Front Genet 9. https://doi.org/10.3389/FGENE.2018.00712.

Charizanis, K., Lee, K.Y., Batra, R., Goodwin, M., Zhang, C., Yuan, Y., Shiue, L., Cline, M., Scotti, M.M., Xia, G., Kumar, A., Ashizawa, T., Clark, H.B., Kimura, T., Takahashi, M. P., Fujimura, H., Jinnai, K., Yoshikawa, H., Gomes-Pereira, M., Gourdon, G., Sakai, N., Nishino, S., Foster, T.C., Ares, M., Darnell, R.B., Swanson, M.S., 2012. Muscleblind-like 2-mediated alternative splicing in the developing brain and dysregulation in myotonic dystrophy. Neuron 75, 437–450. https://doi.org/10.1016/J.NEURON.2012.05.029.

Cioni, J.M., Koppers, M., Holt, C.E., 2018. Molecular control of local translation in axon development and maintenance. Curr. Opin. Neurobiol. 51, 86–94. https://doi.org/10.1016/J.CONB.2018.02.025.

Dincă, D.M., Lallemant, L., González-Barriga, A., Cresto, N., Braz, S.O., Sicot, G., Pillet, L. E., Polvèche, H., Magneron, P., Huguet-Lachon, A., Benyamine, H., Azotla-Vilchis, C. N., Agonizantes-Juárez, L.E., Tahraoui-Boris, J., Martinat, C., Hernández-Hernández, O., Auboeuf, D., Rouach, N., Bourgeois, C.F., Gourdon, G., Gomes-Pereira, M., 2022. Myotonic dystrophy RNA toxicity alters morphology, adhesion and migration of mouse and human astrocytes. Nat. Commun. 13. https://doi.org/10.1038/S41467-022-31594-9.

Fang, C., Manes, T.D., Liu, L., Liu, K., Qin, L., Li, G., Tobiasova, Z., Kirkiles-Smith, N.C., Patel, M., Merola, J., Fu, W., Liu, R., Xie, C., Tietjen, G.T., Nigrovic, P.A., Tellides, G., Pober, J.S., Jane-wit, D., 2019. ZFYVE21 is a complement-induced Rab5 effector that activates non-canonical NF-κB via phosphoinosotide remodeling of endosomes. Nat. Commun. 10. https://doi.org/10.1038/S41467-019-10041-2.

Freyermuth, F., Rau, F., Kokunai, Y., Linke, T., Sellier, C., Nakamori, M., Kino, Y., Arandel, L., Jollet, A., Thibault, C., Philipps, M., Vicaire, S., Jost, B., Udd, B., Day, J. W., Duboc, D., Wahbi, K., Matsumura, T., Fujimura, H., Mochizuki, H., Deryckere, F., Kimura, T., Nukina, N., Ishiura, S., Lacroix, V., Campan-Fournier, A., Navratil, V., Chautard, E., Auboeuf, D., Horie, M., Imoto, K., Lee, K.Y., Swanson, M.S., de Munain, A.L., Inada, S., Itoh, H., Nakazawa, K., Ashihara, T., Wang, E., Zimmer, T., Furling, D., Takahashi, M.P., Charlet-Berguerand, N., 2016. Splicing misregulation of SCN5A contributes to cardiac-conduction delay and heart arrhythmia in myotonic dystrophy. Nat. Commun. 7. https://doi.org/10.1038/NCOMMS11067.

Gallego Romero, I., Pai, A.A., Tung, J., Gilad, Y., 2014. RNA-seq: impact of RNA degradation on transcript quantification. BMC Biol. 12, 42. https://doi.org/10.1186/1741-7007-12-42.

González-Barriga, A., Lallemant, L., Dincă, D.M., Braz, S.O., Polvèche, H., Magneron, P., Pionneau, C., Huguet-Lachon, A., Claude, J.B., Chhuon, C., Guerrera, I.C., Bourgeois, C.F., Auboeuf, D., Gourdon, G., Gomes-Pereira, M., 2021. Integrative cell type-specific multi-omics approaches reveal impaired programs of glial cell differentiation in mouse culture models of DM1. Front. Cell Neurosci. 15. https://doi.org/10.3389/FNCEL.2021.662035.

Goodwin, M., Mohan, A., Batra, R., Lee, K.Y., Charizanis, K., Fernández Gómez, F.J., Eddarkaoui, S., Sergeant, N., Buée, L., Kimura, T., Clark, H.B., Dalton, J., Takamura, K., Weyn-Vanhentenryck, S.M., Zhang, C., Reid, T., Ranum, L.P.W., Day, J.W., Swanson, M.S., 2015. MBNL sequestration by toxic RNAs and RNA misprocessing in the myotonic dystrophy brain. Cell Rep. 12, 1159–1168. https://doi.org/10.1016/J.CELREP.2015.07.029.

Hernández-Hernández, O., Guiraud-Dogan, C., Sicot, G., Huguet, A., Luilier, S., Steidl, E., Saenger, S., Marciniak, E., Obriot, H., Chevarin, C., Nicole, A., Revillod, L., Charizanis, K., Lee, K.Y., Suzuki, Y., Kimura, T., Matsuura, T., Cisneros, B., Swanson, M.S., Trovero, F., Buisson, B., Bizot, J.C., Hamon, M., Humez, S., Bassez, G., Metzger, F., Buée, L., Munnich, A., Sergeant, N., Gourdon, G., Gomes-Pereira, M., 2013. Myotonic dystrophy CTG expansion affects synaptic vesicle proteins, neurotransmission and mouse behaviour. Brain 136, 957–970. https://doi.org/10.1093/BRAIN/AWS367.

Hommersom, M.P., van Prooije, T.H., Pennings, M., Schouten, M.I., van Bokhoven, H., Kamsteeg, E.J., van de Warrenburg, B.P.C., 2022. The complexities of CACNA1A in clinical neurogenetics. J. Neurol. 269, 3094–3108. https://doi.org/10.1007/S00415-021-10897-9.

Jiang, H., Mankodi, A., Swanson, M.S., Moxley, R.T., Thornton, C.A., 2004. Myotonic dystrophy type 1 is associated with nuclear foci of mutant RNA, sequestration of muscleblind proteins and deregulated alternative splicing in neurons. Hum. Mol. Genet 13, 3079–3088. https://doi.org/10.1093/HMG/DDH327.

Jobe, E.M., Zhao, X., 2017. DNA methylation and adult neurogenesis. Brain Plast. 3, 5–26. https://doi.org/10.3233/BPL-160034.

Kanadia, R.N., Johnstone, K.A., Mankodi, A., Lungu, C., Thornton, C.A., Esson, D., Timmers, A.M., Hauswirth, W.W., Swanson, M.S., 2003. A muscleblind knockout model for myotonic dystrophy. Sci. (1979) 302, 1978–1980. https://doi.org/10.1126/SCIENCE.1088583/SUPPL_FILE/KANADIA.SOM.PDF.

Kanda, Y., 2013. Investigation of the freely available easy-to-use software "EZR" for medical statistics. Bone Marrow Transpl. 48, 452–458. https://doi.org/10.1038/BMT.2012.244.

Kim, D., Langmead, B., Salzberg, S.L., 2015. HISAT: a fast spliced aligner with low memory requirements. Nat. Methods 12, 357–360. https://doi.org/10.1038/NMETH.3317.

López-Martínez, A., Soblechero-Martín, P., De-La-puente-ovejero, L., Nogales-Gadea, G., Arechavala-Gomeza, V., 2020. An overview of alternative splicing defects implicated in myotonic dystrophy type I. Genes 2020 Vol. 11. https://doi.org/10.3390/GENES11091109, 1109 11, 1109.

Mankodi, A., Urbinati, C.R., Yuan, Q.P., Moxley, R.T., Sansone, V., Krym, M., Henderson, D., Schalling, M., Swanson, M.S., Thornton, C.A., 2001. Muscleblind localizes to nuclear foci of aberrant RNA in myotonic dystrophy types 1 and 2. Hum. Mol. Genet 10, 2165–2170. https://doi.org/10.1093/HMG/10.19.2165.

Martin, K.C., 2004. Local protein synthesis during axon guidance and synaptic plasticity. Curr. Opin. Neurobiol. 14, 305–310. https://doi.org/10.1016/j.conb.2004.05.009.

Meola, G., Cardani, R., 2015. Myotonic dystrophies: an update on clinical aspects, genetic, pathology, and molecular pathomechanisms. Biochim. Biophys. Acta Mol. Basis Dis. https://doi.org/10.1016/j.bbadis.2014.05.019.

Miller, J.W., Urbinati, C.R., Teng-Umnuay, P., Stenberg, M.G., Byrne, B.J., Thornton, C. A., Swanson, M.S., 2000. Recruitment of human muscleblind proteins to (CUG)n expansions associated with myotonic dystrophy. EMBO J. 19, 4439–4448. https://doi.org/10.1093/EMBOJ/19.17.4439.

Mills, J.D., Kavanagh, T., Kim, W.S., Chen, B.J., Kawahara, Y., Halliday, G.M., Janitz, M., 2013. Unique transcriptome patterns of the white and grey matter corroborate structural and functional heterogeneity in the human frontal lobe. PLoS One 8. https://doi.org/10.1371/JOURNAL.PONE.0078480.

Minnerop, M., Gliem, C., Kornblum, C., 2018. Current progress in CNS imaging of myotonic dystrophy. Front. Neurol. 9. https://doi.org/10.3389/FNEUR.2018.00646.

Mori, Y., Friedrich, T., Kim, M.S., Mikami, A., Nakai, J., Ruth, P., Bosse, E., Hofmann, F., Flockerzi, V., Furuichi, T., Mikoshiba, K., Imoto, K., Tanabe, T., Numa, S., 1991. Primary structure and functional expression from complementary DNA of a brain calcium channel. Nature 350, 398–402. https://doi.org/10.1038/350398A0.

Nakamori, M., Sobczak, K., Moxley, R.T., Thornton, C.A., 2009. Scaled-down genetic analysis of myotonic dystrophy type 1 and type 2. Neuromuscul. Disord. 19, 759–762. https://doi.org/10.1016/J.NMD.2009.07.012.

Nakamori, M., Shimizu, H., Ogawa, K., Hasuike, Y., Nakajima, T., Sakurai, H., Araki, T., Okada, Y., Kakita, A., Mochizuki, H., 2022. Cell type-specific abnormalities of central nervous system in myotonic dystrophy type 1. Brain Commun. 4. https://doi.org/10.1093/BRAINCOMMS/FCAC154.

Nanou, E., Catterall, W.A., 2018. Calcium Channels, Synaptic Plasticity, and Neuropsychiatric Disease. Neuron 98, 466–481. https://doi.org/10.1016/J.NEURON.2018.03.017.

Nishi, M., Kimura, T., Igeta, M., Furuta, M., Suenaga, K., Matsumura, T., Fujimura, H., Jinnai, K., Yoshikawa, H., 2020. Differences in splicing defects between the grey and white matter in myotonic dystrophy type 1 patients. PLoS One 15. https://doi.org/10.1371/JOURNAL.PONE.0224912.

Okkersen, K., Monckton, D.G., Le, N., Tuladhar, A.M., Raaphorst, J., van Engelen, B.G. M., 2017. Brain imaging in myotonic dystrophy type 1: A systematic review. Neurology 89, 960–969. https://doi.org/10.1212/WNL.0000000000004300.

Otero, B.A., Poukalov, K., Hildebrandt, R.P., Thornton, C.A., Jinnai, K., Fujimura, H., Kimura, T., Hagerman, K.A., Sampson, J.B., Day, J.W., Wang, E.T., 2021. Transcriptome alterations in myotonic dystrophy frontal cortex. Cell Rep. 34. https://doi.org/10.1016/J.CELREP.2020.108634.

Romeo, V., Pegoraro, E., Ferrati, C., Squarzanti, F., Sorarù, G., Palmieri, A., Zucchetta, P., Antunovic, L., Bonifazi, E., Novelli, G., Trevisan, C.P., Ermani, M., Manara, R., Angelini, C., 2010. Brain involvement in myotonic dystrophies: neuroimaging and neuropsychological comparative study in DM1 and DM2. J. Neurol. 257, 1246–1255. https://doi.org/10.1007/S00415-010-5498-3.

Saville, D.J., 1990. Multiple comparison procedures: the practical solution. Am. Stat. 44, 174–180. https://doi.org/10.1080/00031305.1990.10475712.

Shen, S., Park, J.W., Lu, Z.X., Lin, L., Henry, M.D., Wu, Y.N., Zhou, Q., Xing, Y., 2014. rMATS: robust and flexible detection of differential alternative splicing from replicate RNA-Seq data. Proc. Natl. Acad. Sci. USA 111, E5593–E5601. https://doi.org/10.1073/PNAS.1419161111.

Suenaga, K., Lee, K.Y., Nakamori, M., Tatsumi, Y., Takahashi, M.P., Fujimura, H., Jinnai, K., Yoshikawa, H., Du, H., Ares, M., Swanson, M.S., Kimura, T., 2012. Muscleblind-like 1 knockout mice reveal novel splicing defects in the myotonic dystrophy brain. PLoS One 7. https://doi.org/10.1371/JOURNAL.PONE.0033218.

Thornton, C.A., Johnson, K., Moxley, R.T., 1994. Myotonic dystrophy patients have larger CTG expansions in skeletal muscle than in leukocytes. Ann. Neurol. 35, 104–107. https://doi.org/10.1002/ANA.410350116.

Weijs, R., Okkersen, K., van Engelen, B., Küsters, B., Lammens, M., Aronica, E., Raaphorst, J., van Cappellen van Walsum, A.M., 2021. Human brain pathology in myotonic dystrophy type 1: a systematic review. Neuropathology 41, 3–20. https://doi.org/10.1111/NEUP.12721.